ACI STRUCTURAL JOURNAL TECHNICAL PAPER

Title no. 94-S65

High-Strength Concrete Columns under Simulated Earthquake Loading


by Oguzhan Bayrak and Shamim A. Sheikh

Main objectives of this research are to evaluate performance of high-strength concrete (HSC) columns for ductility and strength, and to critically examine ACI's Code requirements for confinement steel. Results from four HSC specimens with concrete strength of 72 MPa tested under simulated earthquake loading are presented here and compared with similar specimens made of normal strength concrete, (NSC). Each specimen consisted of a 305 × 305 × 1473 mm column and 508 × 762 × 813 mm stub which represented a discontinuity like a beam column joint or a footing.

The variables studied in this research are the concrete strength, steel configuration, axial load level, amount of lateral steel, and the presence of a heavy stub. As in the case of normal strength concrete, an increase in the amount of lateral steel, reduction in axial load, and increased effectiveness of the lateral support provided to longitudinal bars resulted in increases in energy absorption and dissipation capacity as well as ductility. For a specified column performance if the axial load measured as a fraction of P_o is kept constant, the required amount of lateral steel appears to be proportional to the strength of concrete, in the 30 to 72 MPa strength range considered in this study.

Keywords: deformability; ductility; energy dissipation capacity high-strength concrete; member performance; sectional performance; stiffness; strength; tied columns.

INTRODUCTION

The response of most structures designed according to the current seismic design philosophy and subjected to severe earthquake is not expected to be elastic. Allowing some inelastic deformations to take place and using a reduced base shear force, rather than the base shear corresponding to elastic response has been preferred for economic reasons. Hence, the ability of a structure to withstand a severe earthquake depends mainly on the formation of plastic hinges and their capacities to absorb and dissipate energy without significant loss of strength. To ensure stability as well as the vertical load carrying capacity while structures undergo large lateral displacements, most of the building codes attempt to produce hinging in the beams rather than in the columns. However, recent earthquakes and analytical investigations[1,2] showed that formation of plastic hinges in columns is still possible as a result of strong ground motion despite the application of "strong column-weak beam" concept, as recommended by various design codes. Besides, at the column bases of multi-story frames and in bridges column hinging is unavoidable, in fact should be relied on for energy dissipation.

The use of high-strength concrete, HSC, has become widespread over the last 10 to 15 years. For seismic and non-seismic design, higher concrete strength and higher modulus of elasticity generally result in smaller cross-sections and therefore substantial savings. However, the use of HSC in seismic regions necessitates extra caution to ensure the desired ductile behavior.

The work presented here is part of a comprehensive research[2-7] program which aims to study confinement of concrete by circular as well as rectilinear lateral reinforcement. The current work deals with the experimental behavior of reinforced concrete columns confined by rectilinear ties and subjected to axial load and cyclic flexure and shear simulating earthquake loads. In an earlier study,[3] similar large-size normal strength concrete, NSC, specimens were tested under similar loading conditions. A comparison of current test results with those from the previous studies allows a direct evaluation of the effect of concrete strength in addition to the variables such as steel configuration and level of axial load on the behavior of columns.

RESEARCH SIGNIFICANCE

Design equations containing empirical constants which can be found in most reinforced concrete design codes[8,9,10] are based mostly on experimental work in which normal strength concrete was used. This necessitates the evaluation of the applicability of such equations to high strength concrete. Moreover, North American Design Codes[8,9] require-

ACI Structural Journal, V. 94, No. 6, November-December 1997.
Received November 15, 1995, and reviewed under Institute publication policies.
 Pertinent discussion will be published in the September-October 1998 *ACI Structural Journal* if received by May 1, 1998.

Oguzhan Bayrak is a PhD candidate in the Department of Civil Engineering at the University of Toronto. He received his MASc degree from the University of Toronto in 1995. His research interests include earthquake resistant design of reinforced concrete members and structures, in particular columns, dynamic analysis of bridges, and elevated viaducts and repair of delaminated reinforced concrete columns with ACM.

Shamim A. Sheikh is a professor of civil engineering at the University of Toronto. He is the chairman of joint ACI-ASCE Committee 441, Reinforced Concrete Columns; and a member of 442, Response of Concrete Buildings to Lateral Forces. His research interests include confinement of concrete, earthquake resistance of reinforced concrete, expansive cement and its application to deep foundation, and repair of delaminated reinforced concrete columns with ACM.

ments for the design of confinement steel do not consider important factors, such as the level of the axial load and the steel configuration. In the event of large inelastic displacement demands, the code procedure for confinement steel would result in an undesirable brittle column behavior in many cases particularly for columns under high axial loads. For less severe conditions or less ductile performance demands, the confinement steel design according to these codes[8,9] would be unnecessarily conservative for well-configured columns. A more rational design procedure has been suggested recently[11] for the design of confinement steel in concrete with strength up to 55 MPa. Very limited amount of data from realistically sized HSC specimens tested under realistic conditions is available today. With the ever increasing use of HSC in practice, test data on HSC behavior is needed to evaluate the performance of structures and check the validity of the suggested procedure and, if necessary, develop new guidelines or suggest modifications to existing ones. This paper presents results from an experimental study to partially meet this requirement.

EXPERIMENTAL PROGRAM

Results from four large-scale reinforced concrete column specimens made from 72 MPa concrete and tested under constant axial load and large cyclic inelastic lateral displacements are presented. These results are compared with those from earlier tests[3,5,6] on similar specimens having concrete strengths between 31 and 55 MPa. The level of the axial load, as measured by index P/P_o, varied from 0.36 to 0.50. Relatively high axial loads are used in the test program because most of the design codes allow high axial loads and there is only a limited amount of test data available for large-size HSC specimens tested under these levels of axial load and cyclic lateral load.

Specimens

Each specimen consisted of a 305 × 305 × 1473 mm column cast integrally with a 508 × 762 × 813 mm stub. The column part of the specimen represents the part of a column in a regular building frame between the section of maximum moment and the point of contraflexure. The stub represents a discontinuity like a beam-column joint or a footing adjacent to the section of maximum moment. The core size measured from the center of the perimeter tie was kept constant at 267 × 267 mm for all the specimens, giving a core area equal to 77 percent of the gross area of the column. Table 1 includes details of the test specimens. Each specimen contained 8-20M longitudinal bars providing reinforcement ratio of 2.58 percent of the gross cross-sectional area of the column. Yield strength of the longitudinal steel was 454 MPa. The first letter in the specimen designations indicates the steel configuration. In A-type specimens, four corner longitudinal bars were supported by bends in perimeter hoops and middle longitudinal bars were supported by internal diamond hoops; whereas in E-type specimens, only four corners bars were laterally supported (Fig. 1). Volumetric ratio of rectilinear ties to concrete core, measured center-to-

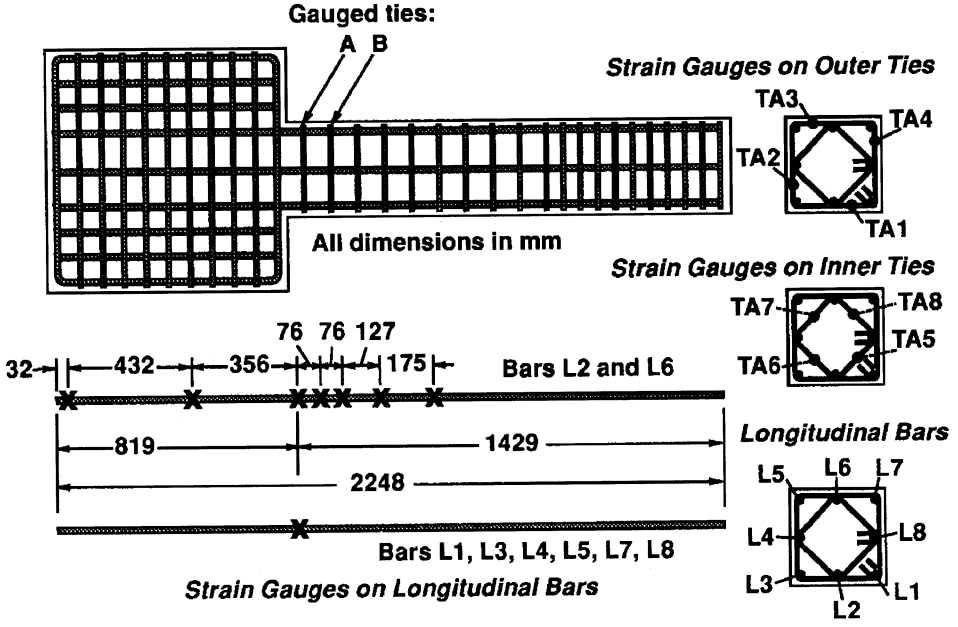

Fig. 1—Location of strain gauges

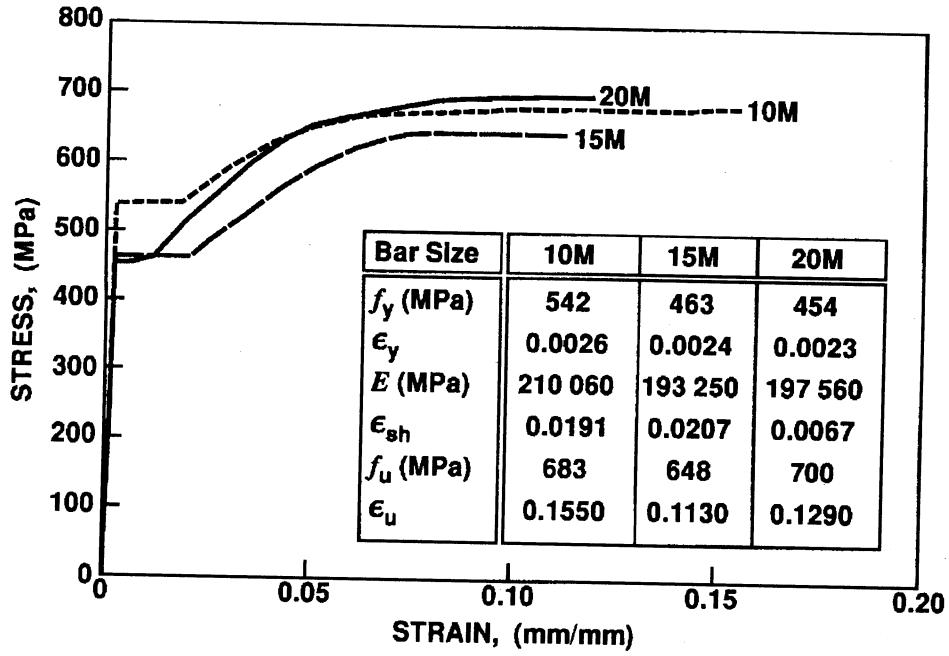

Fig. 2—Stress-strain behavior of steel

Table 1—Member and section ductility parameters

Specimen	$R_{A/P}$	f'_c, MPa	Lateral steel: size at spac., mm	Lateral steel: ρ_s, percent	Lateral steel: f_{yh}, MPa	Lateral steel: $\frac{A_{sh}}{A_{sh(ACI)}}$	Axial load: $\frac{P}{f_c'A_g}$	Axial load: $\frac{P}{P_o}$	Ductility factor: μ_Δ $0.8P_{max}$	Ductility factor: μ_ϕ $0.8M_{max}$	Ductility factor: μ_ϕ $0.9M_{max}$	Ductility ratios: $N_{\Delta 80}$	Ductility ratios: $N_{\Delta t}$	Ductility ratios: $N_{\phi 80}$	Ductility ratios: $N_{\phi t}$	Energy indicators: W_{80}	Energy indicators: W_t	Energy indicators: E_{80}	Energy indicators: E_t
ES-1HT	2.3	72.1	15M at 95	3.15	463.0	1.13	0.50	0.50	4.6	6.6	5.9	15	20	19	25	33	57	80	105
AS-2HT	3.3	71.7	10M at 90	2.84	542.0	1.19	0.36	0.36	6.2	15.8	13.6	18	61	53	113	41	313	631	1412
AS-3HT	2.4	71.8	10M at 90	2.84	542.0	1.19	0.50	0.50	5.0	10.1	9.1	15	28	20	42	36	102	161	396
AS-4HT	3.7	71.9	15M at 100	5.12	463.0	1.83	0.50	0.50	7.0	21.2	17.7	25	69	84	151	231	354	997	1688
AS-18H	2.4	54.7	#4 at 108	3.06	464.0	1.44	0.64	0.61	3.9	14.0	11.0	19	23	43	59	53	54	384	458
AS-17	2.4	31.3	#3 at 108	1.68	507.4	1.52	0.77	0.63	3.8	12.0	10.5	24	30	52	58	58	76	402	443
ES-13	2.1	32.5	#4 at 114	1.69	436.6	1.34	0.76	0.63	2.0	6.0	2.5	7	10	15	26	9	14	53	110

center of perimeter tie, varied between 2.84 percent and 5.12 percent, and spacing of the ties varied with in a narrow range of 90 mm to 100 mm.

Concrete

Ready-mix normal weight concrete with an average slump of 135 mm was used. Forty-eight standard cylinders were cast with the specimens and tested frequently to monitor the strength of concrete. The 7-day strength of concrete was about 87 percent of the 28-day strength and after the 28th day concrete strength increased by about 10 percent in the following six months. The concrete strength of each specimen (Table 1) was obtained from the strength-versus-age relationship developed.

Steel

Three different types of reinforcing steel were used to construct specimens. 10M and 15M bars were used for the ties and 20M size was used for the longitudinal bars. Stress-strain curves of steel in tension are given in Fig. 2. Each curve represents an average of three test results. Important properties of steel are also listed in the figure. ε_y, ε_{sh}, ε_u represent strain values at the onset of yield, at the initiation of strain hardening, and at rupture respectively; f_y and f_u are the yield strength and ultimate strength, respectively.

Reinforcing cages

The reinforcement for the stub consisted of 10M horizontal and vertical stirrups at 64 mm spacing. The longitudinal bars in columns were extended through the stub to 20 mm

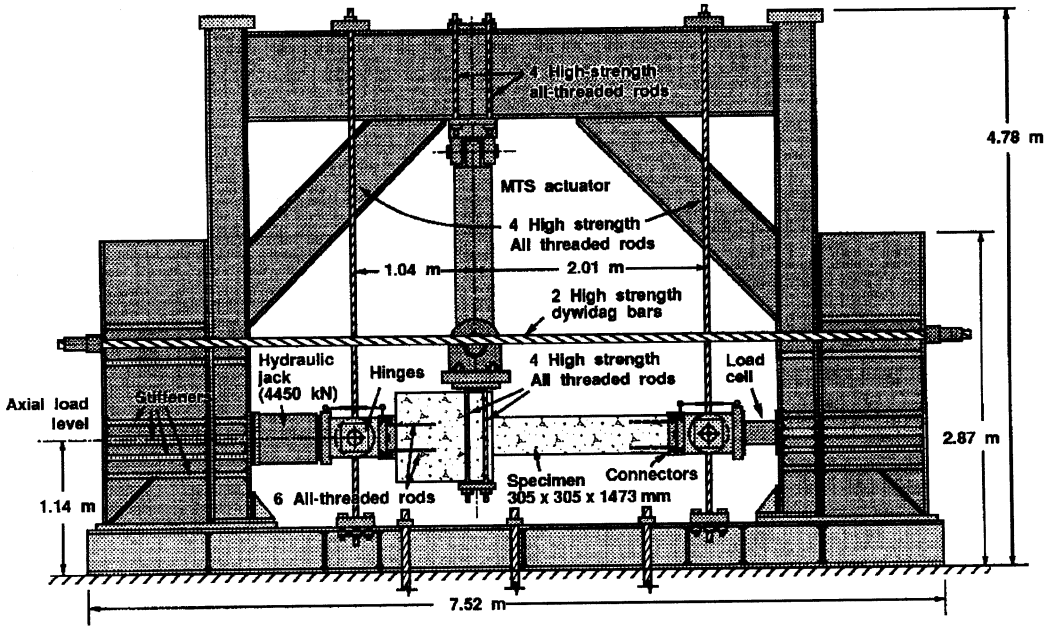

Fig. 3—Schematic of the test setup

from the ends in all specimens. The ties were placed at predetermined spacing within the 910 mm long test regions of the columns adjacent to the stubs. Beyond that point, the spacing was reduced to half of predetermined value to provide extra confinement and reduce chances of failure there. Two different steel configurations (Fig. 1) were used in the test regions of the columns. Minimum anchorage of ties conformed to the ACI Building Code requirements.[8] No anchorage failure was observed in any specimen.

Instrumentation

Concrete and steel strains at various locations, deflections along the specimen length and axial and lateral loads were monitored during each test through the use of extensive instrumentation. Figure 1 also shows the locations of strain gauges on longitudinal and lateral steel. Two sets of ties in the column closest to the stub were instrumented with strain gauges. A-type specimens had a total of 36 strain gauges, whereas 28 strain gauges were used in E-type specimen. Longitudinal concrete strains in the core were measured by using linear variable differential transducers (LVDTs) over gauge lengths that ranged from 51 to 102 mm and covered a length of about 460 mm from the column-stub interface. Transverse deflections at six locations along the length of the specimens were measured using LVDTs. Shear deformation in the plastic hinge region was also measured through the use of two diagonally placed LVDTs. A total of 24 LVDTs were employed in each test.

Testing

All the specimens were tested under constant axial load and reversed cyclic displacement excursions in the test frame illustrated in Fig. 3. All specimens except AS-2HT were loaded downward first. A 4450 kN hydraulic jack and a load cell of similar capacity were used to apply and measure the axial load. Optical measurement devices were used for the

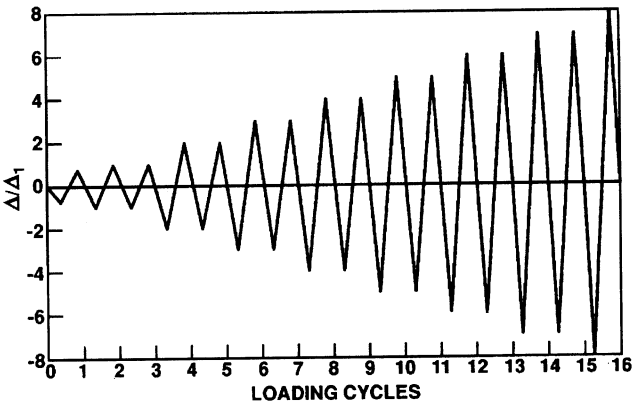

Fig. 4—Specified displacement history

preliminary alignment of the specimen. To check the alignment, axial load was applied in 250 kN intervals and the strain gauges and LVDTs were monitored regularly. In most specimens, very little adjustment was required for the alignment, but when necessary the specimen was unloaded for adjustment. After the final positioning, the alignment was checked up to the maximum predetermined axial load; and the lateral load actuator was connected to the specimen after applying the full axial load. The specimen was then subjected to predetermined displacement excursions (Fig. 4). In the first cycle the specimen was subjected to 75 percent of the elastic or yield displacement (Δ_1), which can be defined as the lateral deflection corresponding to the estimated lateral load carrying capacity (P_{max}) on a straight line joining origin and a point about 65 percent of P_{max} on the lateral load-displacement curve. It should be recognized that, both Δ_1 and P_{max} were calculated using the theoretical sectional response of the unconfined column and integrating curvatures along

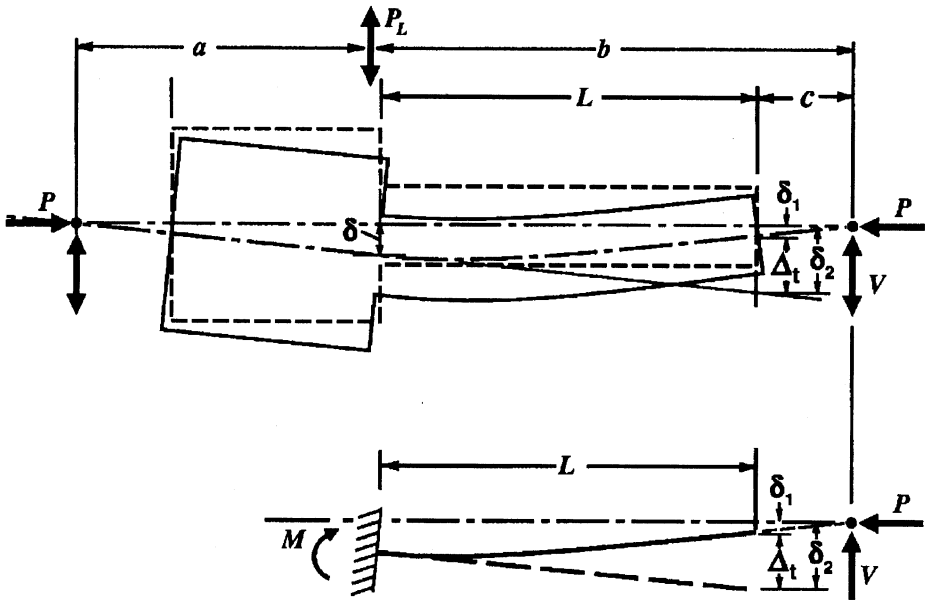

Fig. 5—Idealization of specimens

the length of the specimen. Moment generated by the axial load was not considered in the calculation of Δ_1 since this effect is minimal in the earlier stages of column response. The specimen was subjected to increasing reversed cyclic displacement excursions until it was unable to maintain the originally applied axial load.

TEST RESULTS

Behavior of each specimen is presented graphically in the form of column shear force versus tip deflection and moment versus curvature relationships. Fig. 5 shows the idealization of a specimen and the definitions of shear force V, and tip deflection Δ_t used in Figs. 6 to 9. The deflection at the failed section was determined from the measured deflected shape of the column, and was used to calculate secondary moment due to axial load. The curvature was calculated from the deformation readings measured by the upper and lower LVDTs located in the most damaged region within the hinging zone. The gauge lengths were kept constant in all the specimens. Spalling of top and bottom cover concrete, yielding of perimeter tie, and buckling of top and bottom longitudinal bars are marked on the graphs in Figs. 6 to 9. In all the specimens failure did not occur at the column stub connection, although this section was subjected to the maximum moment. Due to the additional confinement provided by the stub to the adjacent column section, the failure shifted away from the stub.

Test observations

First signs of distress in all of the tested specimens were the cracks in the top and bottom concrete cover. The number of cracks formed and their lengths increased in the first three cycles as the number of displacement excursions to which specimens were subjected, increased. For Specimens AS-2HT, AS-3HT, and AS-4HT top concrete cover spalled off suddenly at the first downward peak of the fourth cycle ($\Delta = 2\Delta_1$), and the bottom concrete spalled off in the second peak of the same cycle. For Specimen ES-1HT, on the other hand, top concrete cover spalled off at the first peak of the fourth cycle ($\Delta = 2\Delta_1$), and bottom concrete cover severely cracked in the same cycle and spalled off in the next cycle. The concrete strain at the time of spalling of cover concrete was 0.0026, 0.0024, 0.0022, 0.0023, respectively for Specimens ES-1HT, AS-2HT, AS-3HT, and AS-4HT. After the sixth cycle ($\Delta = 3\Delta_1$), cracking propagated to the sides of the column and at later stages, spalling of the cover concrete at the sides of the specimen was observed. Vertical flexural cracks formed first in the hinging zones at a distance of approximately 200 mm to 350 mm from the face of the stub and extended further in later stages towards the stub. The most extensive damage concentrated at about 180 mm to 240 mm from the column-stub interface, in the four specimens. Spalling of cover extended from close to the stub for a distance which varied between about 400 mm and 750 mm in different specimens.

In most cases, during the last cycle buckling of the longitudinal bars was observed after yielding of the perimeter ties, which was an indication of the commencement of failure. At the initiation of buckling of longitudinal bars, the maximum concrete compressive strain at core was respectively 0.008, 0.012, 0.011, and 0.012 for Specimens ES-1HT, AS-2HT, AS-3HT, and AS-4HT. The maximum concrete compressive strains at core just before the failure was 0.015, 0.020, 0.018, and 0.025 for Specimens ES-1HT, AS-2HT, AS-3HT, and AS-4HT, respectively. The failure of the specimen was accompanied by extensive buckling of the longitudinal bars in all the specimens. In Specimen AS-3HT some of the buckled bars fractured. No pinching of the force-deformation loops (Figs. 6 to 9) was observed in any of the specimens. The failure mode for all of the specimens was dominated by flexural effects.

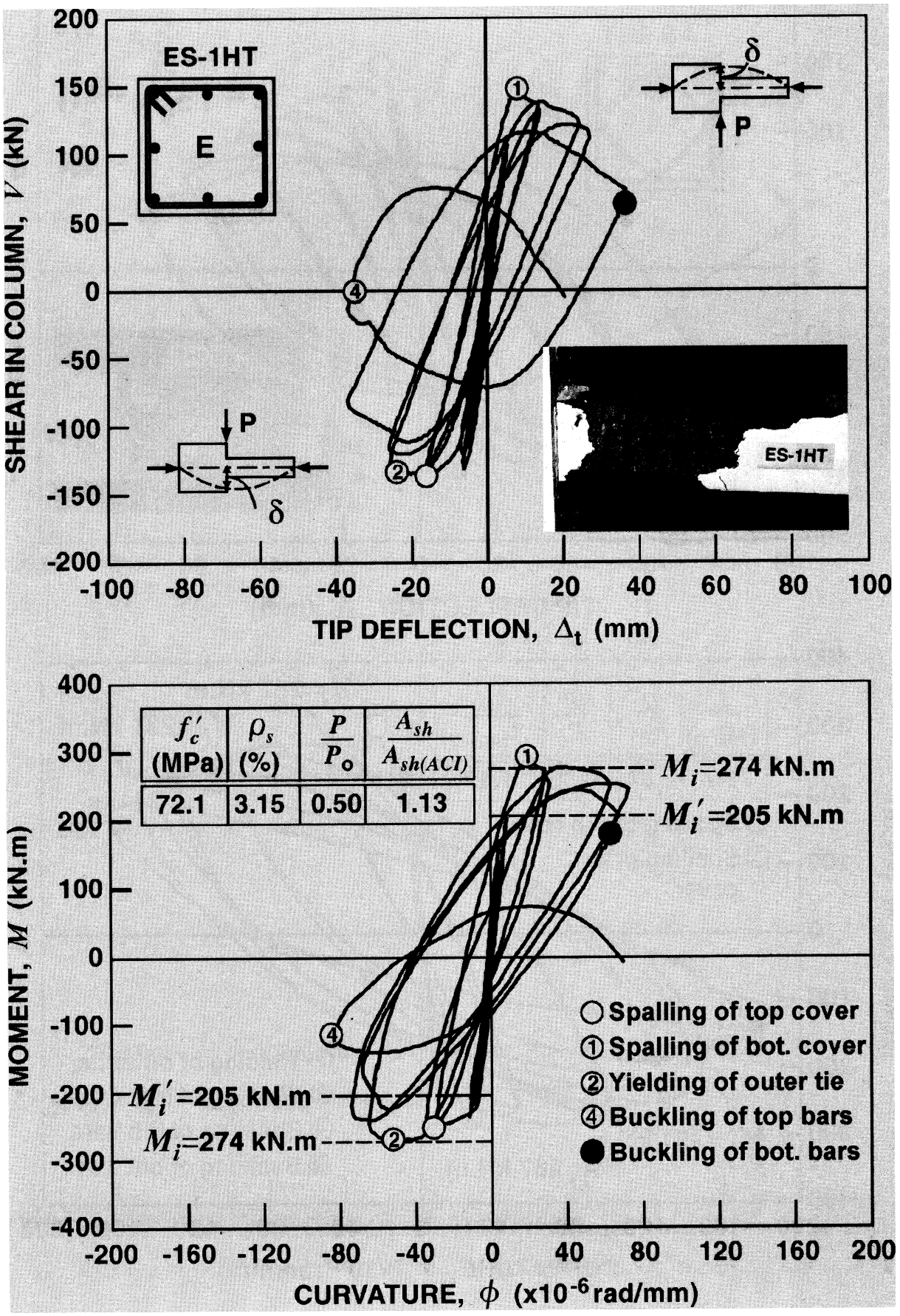

Fig. 6—Behavior of Specimen ES-1HT

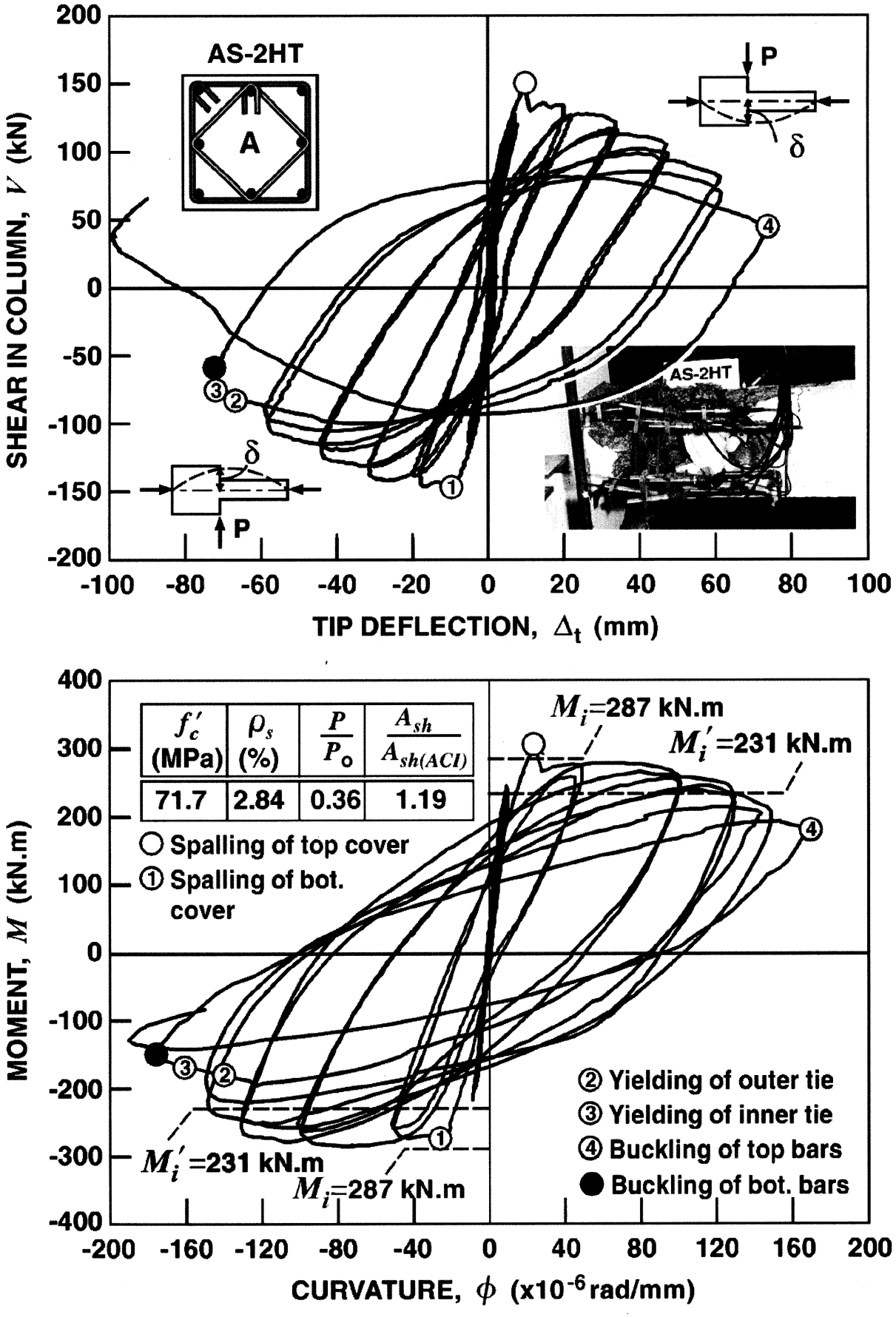

Fig. 7—Behavior of Specimen AS-2HT

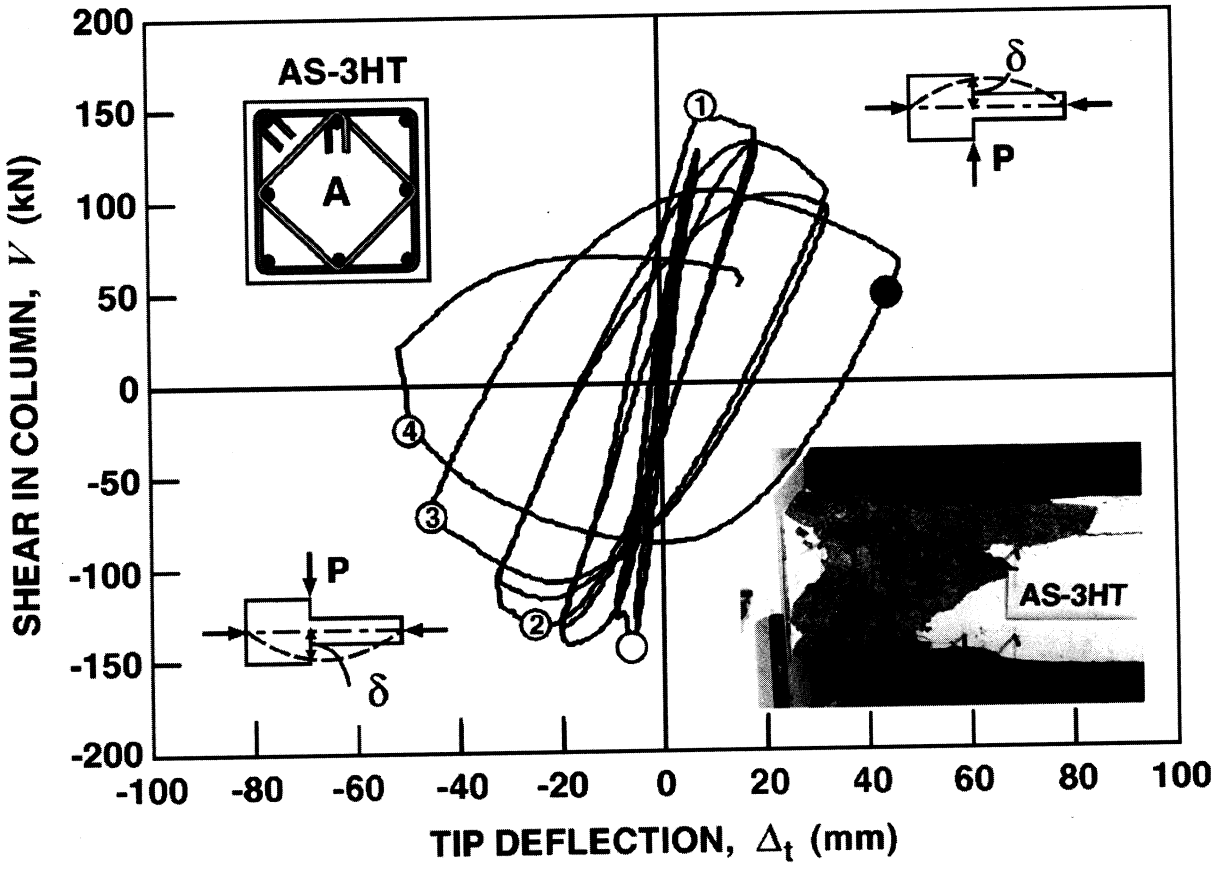

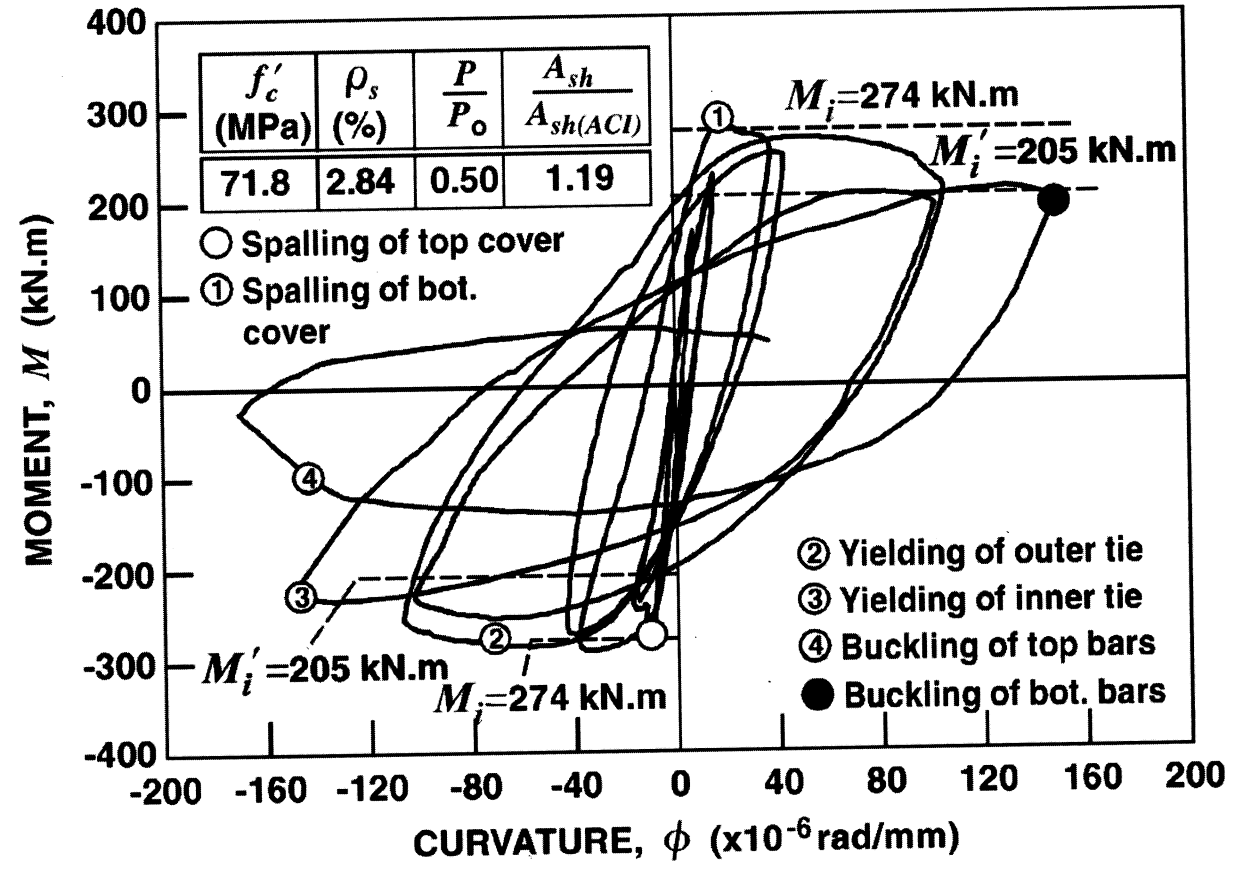

Fig. 8—Behavior of Specimen AS-3HT

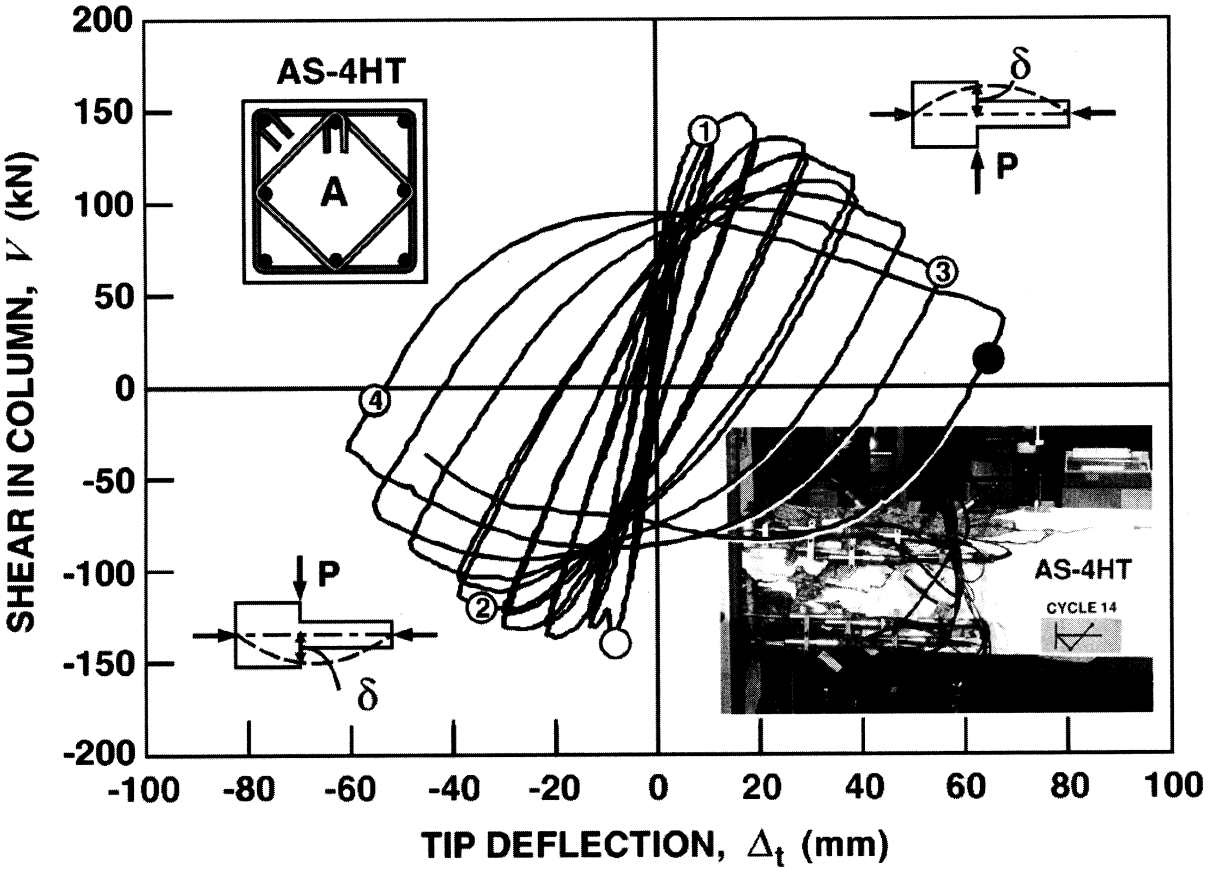

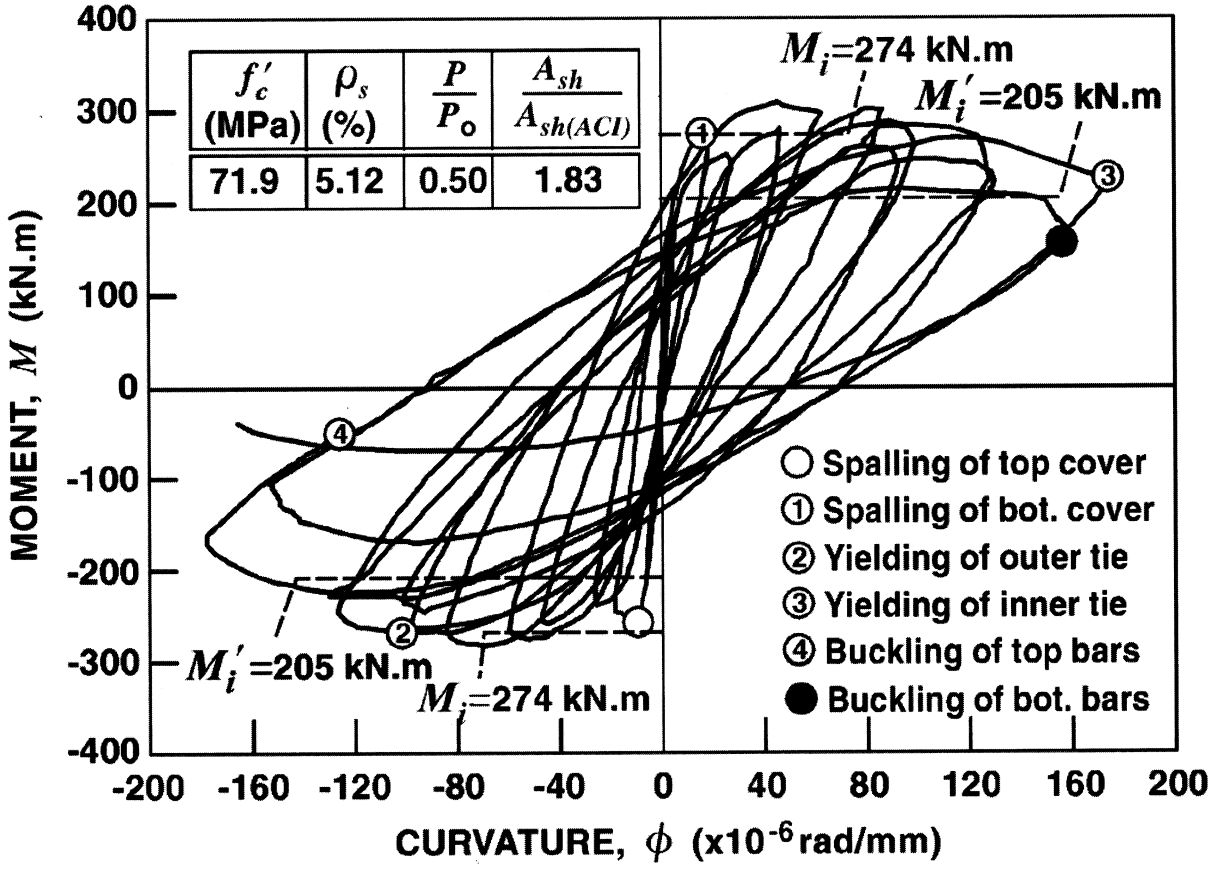

Fig. 9—Behavior of Specimen AS-4HT

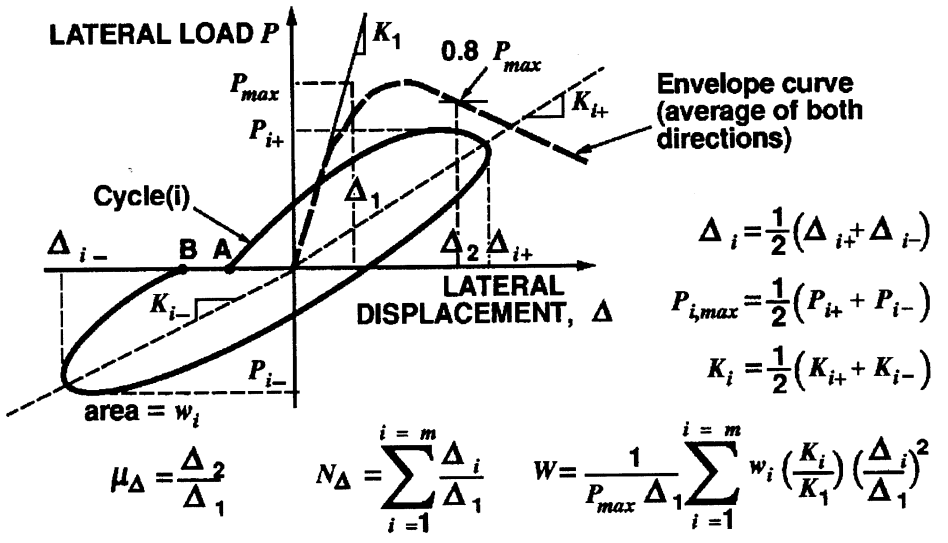

(a) Member Ductility Parameters

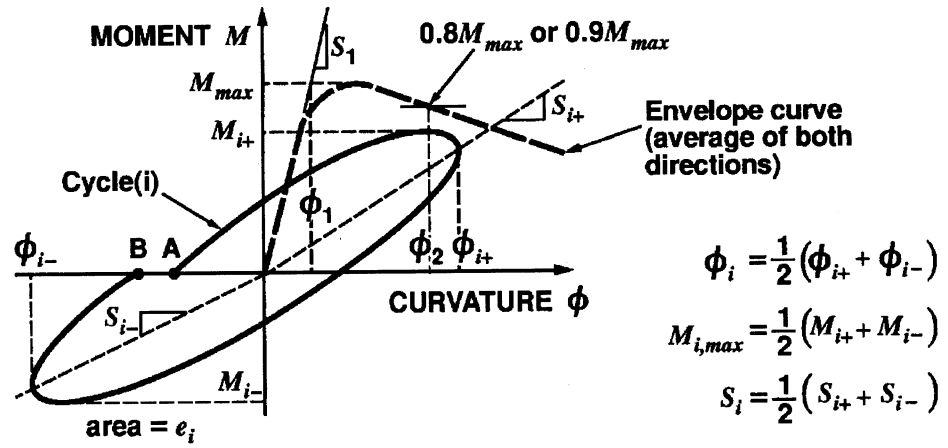

(b) Section Ductility Parameters

Fig. 10—Definitions of ductility parameters

Definitions of ductility parameters

Since the behavior of reinforced concrete sections and members is not elastic-perfectly plastic, several definitions for ductility and deformability are available in the literature. In this study the ductility parameters suggested by Sheikh and Khoury[5] are used to evaluate the performance of the specimens which makes the comparison of test results from the current study to those from earlier similar studies more rational.

Fig. 10 describes various ductility parameters that include curvature and displacement ductility factors μ_ϕ and μ_Δ, cumulative ductility ratios N_ϕ and N_Δ, energy damage indicator E, and work damage indicator W. Subscripts t and 80 are added, respectively, to N_ϕ, N_Δ, E, and W to indicate the value of each parameter until the end of the test, and until the end of the cycle in which the shear force or the moment is dropped to approximately 80 percent of the maximum value, and which is followed by a cycle in which the capacity loss is significantly greater than 20 percent. All the terms are defined in Fig. 10 except L_f and h, which represent, respectively, the length of the most damaged region measured during the test and the depth of the column section. The ductility factors and cumulative ductility ratios represent the deformability of the section or member; whereas the damage indicators estimate toughness. The work damage indicator W used in this study is similar to the one proposed by Ehsani and Wight.[12] Table 1 lists the ductility parameters for the specimens tested in the current study and also for those tested earlier to provide a basis of comparison between NSC specimens and HSC specimens.

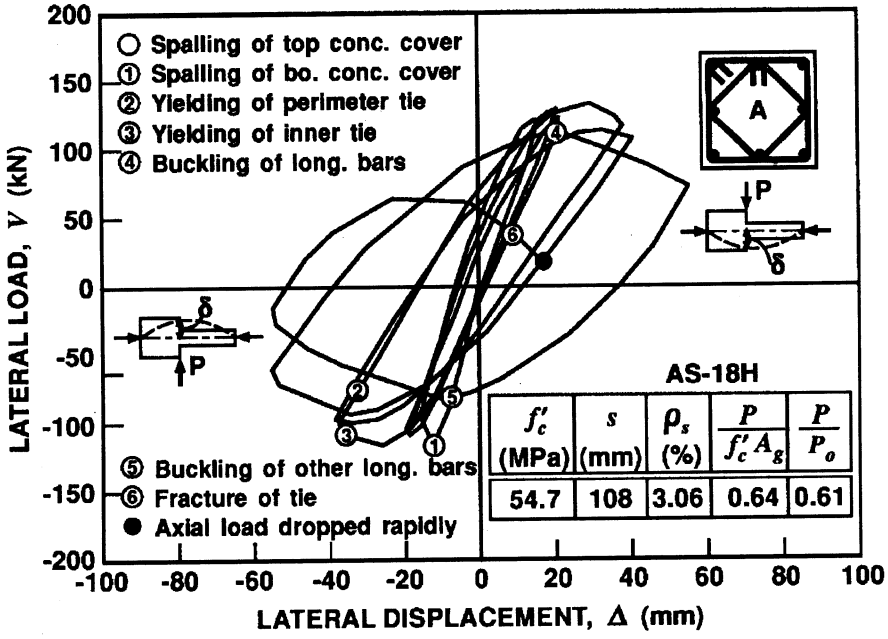

(a) Lateral Load vs. Deflection Behaviour

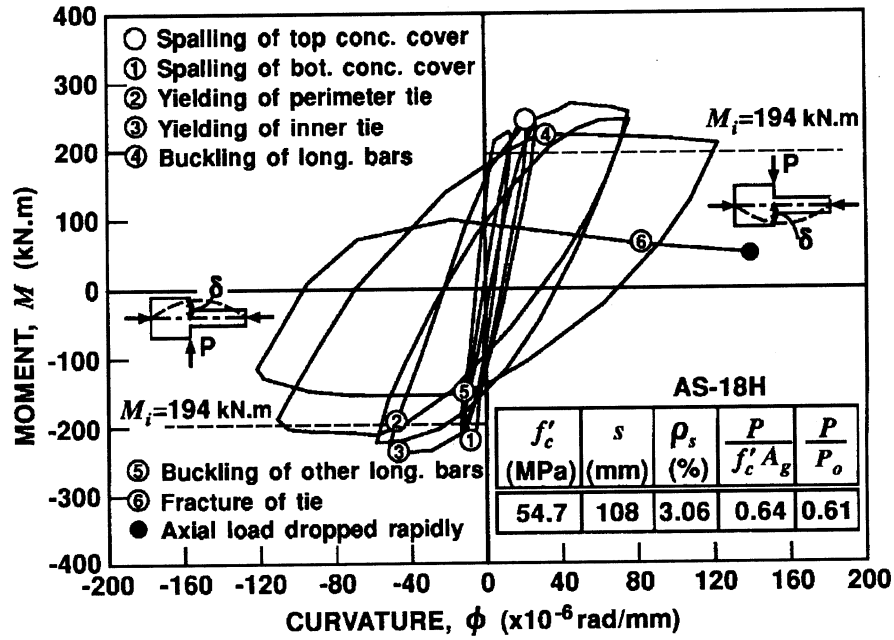

Fig. 11—Behavior of Specimen AS-18H

DISCUSSION OF RESULTS

A general study of Fig. 6 to 9 indicates that HSC columns ($f_c' \approx 72$ MPa) can be made to behave in a ductile manner under high levels of axial load, provided that sufficient amount of confining steel is used in an efficient configuration. Specimen AS-4HT which had 83 percent more steel than the ACI 318-89[8] requirements behaved in a highly ductile manner, showing a displacement ductility factor (μ_Δ) of 7 and curvature ductility factor ($\mu_{\phi 80}$) of over 21. The noticeable differences between the responses of the tested specimens (Figs. 6 to 9) indicate that confinement is affected greatly by different variables. Sectional behavior represented by the M-ϕ relationship of all the specimens is of primary concern here because the deformations concentrate at the plastic hinge region once the column is loaded in the post-elastic range and further lateral displacements will take place mainly as a result of plastic hinge rotation.

Effect of concrete strength

Specimens AS-3HT, AS-18H, and AS-17 can be compared to evaluate the influence of concrete strength on column behavior (Fig. 8, 11, 12, and Table 1). The variable $R_{A/P}$ used in this table is defined[2] as follows;

$$R_{A/P} = \frac{A_{sh}/A_{sh(ACI)}}{P/P_o} \quad (1)$$

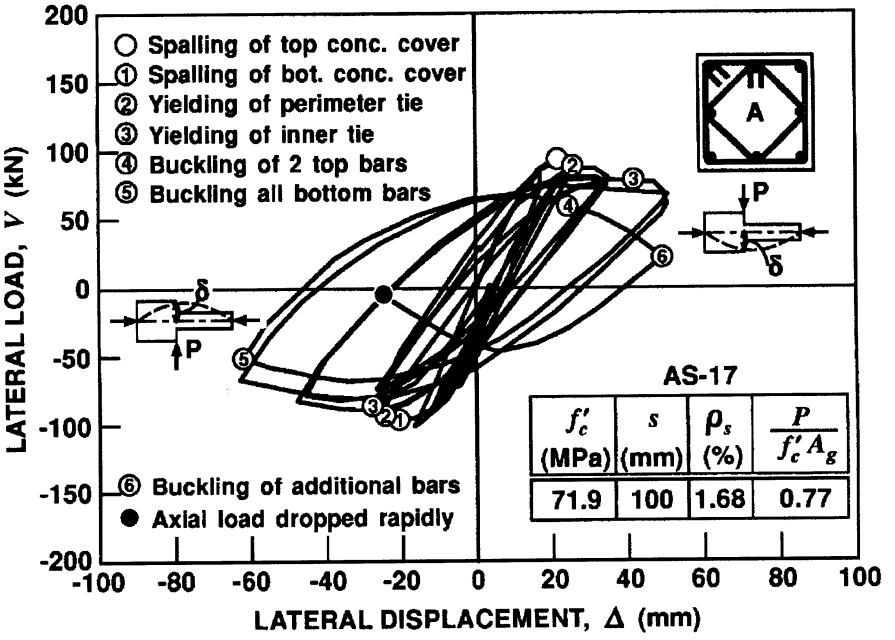

(a) Lateral Load vs. Deflection Behaviour

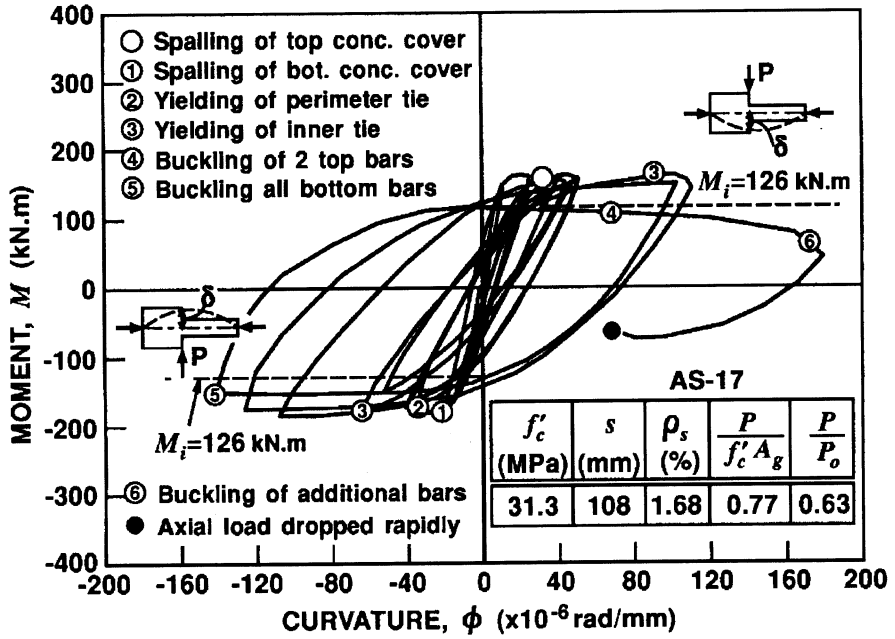

Fig. 12—Behavior of Specimen AS-17

It is believed that specimens having the same $R_{A/P}$ ratios, and the same type of lateral steel configuration are comparable. In this expression the level of axial load is presented by the index variable P/P_o rather than the index $P/f_c'A_g$. For columns with similar f_c', both these indices provide similar comparison; whereas for different f_c' values in columns the comparison may not remain valid with index $P/f_c'A_g$. The required amount of lateral steel was observed to be proportional to the strength of concrete for a certain column performance if the axial load is measured as a fraction of P_o rather than $f_c'A_g$.[6] Specimens AS-17 and AS-18H are tested under very similar levels of axial load (P/P_o = 0.63 and 0.61, respectively) and they satisfied the ACI 318-89[8] code requirements for the amount of confinement steel approximately to the same degree ($A_{sh}/A_{sh(ACI)}$ = 1.52 and 1.44, respectively). Specimen AS-3HT, on the other hand, tested at a lower level of axial load (P/P_o= 0.50) and contained 19 percent more steel than the Code's[8] requirements. As a result, the $R_{A/P}$ ratios are very similar in all three specimens. An examination of moment-curvature behavior of these specimens (Fig. 8, 11, and 12) and a comparison of ductility parameters in Table 1 indicate that despite the large differences in their concrete strength, all the specimens displayed similar behavior. An examination of $\mu_{\phi 90}$, $N_{\phi 80}$, E_{80}, and $N_{\Delta 80}$, W_{80}, indicate that the higher strength concrete specimens have lower deformability and energy absorption ca-

pacities initially, but during the later part of the displacement excursions, these properties improve rapidly and the total values are comparable to those of lower strength concrete specimens. A similar conclusion can be drawn from a comparison of section ductility parameters (μ_ϕ, N_ϕ, E) for Specimens ES-13, and ES-1HT shown in Table 1. Moment-curvature response for ES-13 is available elsewhere.[3]

Effect of steel configuration

Effect of steel configuration on the cyclic behavior of HSC columns can be examined by comparing the behavior of specimens ES-1HT and AS-3HT which contained 13 percent and 19 percent more steel than ACI 318-89[8] requirements, respectively, and were tested under the same level of axial load. Curvature ductility factors ($\mu_{\phi 80}$ and $\mu_{\phi 90}$) of Specimen AS-3HT are approximately 55 percent larger than those of Specimen ES-1HT. Similarly $N_{\phi t}$ value of AS-3HT is 68 percent larger than that of ES-1HT and total energy dissipated in Specimen AS-3HT, measured by E_t, is 3.8 times as much as the energy dissipated in Specimen ES-1HT. Similar conclusions can be drawn from a comparison of member ductility parameters (Table 1). Lower efficiency of confinement in "E" configuration, early buckling of middle longitudinal bars of Specimen ES-1HT and subsequent loss of confinement are the main reasons behind its relatively less ductile behavior. Specimen ES-1HT which had 13 percent more steel than the ACI 318-89 Code's requirements displayed poor energy absorption and dissipation characteristics and behaved in a brittle manner. There was little warning before the failure of this specimen unlike the Specimen AS-3HT. Better distribution of steel and better lateral support to the longitudinal bars provided tougher response of HSC columns, an effect similar to the one observed for NSC columns.[3]

The current design codes' [8,9,10] requirements for the design of confinement steel do not relate the required amount of lateral steel to steel configuration. In other words, the use of Configurations A and E in columns is allowed, and no differentiation is made between the efficiency of confinement in each configuration. Results of current experimental study supports the need to incorporate steel configuration as a design parameter to existing concrete design codes' requirements for confinement steel.

Effect of axial load

Specimens AS-2HT and AS-3HT are similar in every respect except that P/P_o is 0.36 for Specimen AS-2HT and 0.50 for Specimen AS-3HT. Both specimens contained the same amount of lateral steel which is about 19 percent more than the ACI Code[8] requirements. Shear force-tip deflection and moment-curvature relationships of the failed sections of the two specimens are shown in Figs. 7 and 8, and member and section ductility parameters calculated based on these curves are listed in Table 1. An increase in axial load from $0.36P_o$ to $0.50P_o$ caused substantial reductions in the curvature ductility factors, $\mu_{\phi 80}$ and $\mu_{\phi 90}$. Moreover, the cumulative curvature ductility ratios showed significant reductions, from 53 to 20 for $N_{\phi 80}$ and 113 to 42 for $N_{\phi t}$ as a result of increased load. Similar conclusions can be drawn through the comparison of the energy damage indicators, E_{80} and E_t; in fact, energy damage indicators appear to be affected most compared to the other parameters. The energy dissipated in Specimen AS-2HT measured by E_{80} and E_t, is 3.6 to 4 times as much as the energy dissipated in Specimen AS-3HT. Reductions of 19 percent, 54 percent and 67 percent were observed in displacement ductility factor, μ_Δ, cumulative displacement ductility ratio, $N_{\Delta t}$, and work-damage indicator, W_t, respectively, due to the increase in axial load.

A higher axial load resulted in an increase in the rate of stiffness degradation with every load cycle and adversely affected the cyclic performance of HSC columns. These results underlined the need to incorporate the level of axial load in computing the required amount of confining steel.

Effect of amount of lateral steel

Specimens AS-3HT and AS-4HT can be compared to evaluate the effect of the amount of lateral steel on cyclic behavior of columns. Moment-curvature relationships of the failed sections of these specimens, and their shear force-tip deflection curves, are shown in Figs. 8 and 9. These two specimens tested under the same level of axial load, have the same concrete strength, and same steel configuration, but contain different amounts of lateral steel. Volumetric ratio of tie steel to concrete core, ρ_s, for AS-4HT is 80 percent greater than that of AS-3HT. An increase in the amount of lateral steel significantly improved the cyclic behavior of the specimen. The section moment capacity was still increasing after the spalling of cover concrete in Specimen AS-4HT, indicating an excellent confinement of the concrete core. Both the stiffness degradation and strength reduction rate with every load cycle were lower for Specimen AS-4HT compared to Specimen AS-3HT. All the member and section ductility parameters of Specimen AS-4HT are also significantly higher (Table 1). For instance, the energy dissipated in Specimen AS-4HT measured by E_{80} and E_t is 4.3 to 6.2 times as much as the energy dissipated in Specimen AS-3HT.

Stub effect

It is known that the maximum moment in the column occurred at the column-stub interface. However, in each specimen the failure started at a section away from the face of the stub indicating that the strength of the critical section at the column-stub interface was higher than that of the failed section due to the additional confinement provided by the stub which caused a delay of spreading of cracks in concrete and reduced the tendency of lateral expansion. As a result of the increased moment capacity of the critical section, failure shifted to a nearby section. Fig. 13 shows the most damaged regions of the columns in the specimens tested during this study. The center of the most damaged zone is approximately 264 mm away from the column-stub interface as an average for these four specimens. In the capacity design approach for earthquake resistance, appropriate corrections should therefore be made when calculating design shear in columns where the critical sections are adjacent to beam-column joints, and other discontinuities. If the actual flexural capacity of the section is unknown, the shear force should be based on the moment capacities of the plastic hinges and the distance between them; which is about h to $2h$ less than the column length, where h is the column depth.

Experimental moment capacities, M_{exp}, of the failed sections in the extensively damaged regions nearest to the stub are calculated as an average of both loading directions and presented in Table 2. M_i is the theoretical moment capacity calculated using actual stress-strain relationship for HSC, and actual steel properties. M_{ACI} is the moment capacity calculated using the ACI Code[8] provisions for concrete stress block and actual steel properties. During testing it was observed that cover concrete spalled suddenly in most of the specimens and the concrete strain at the time of spalling of top cover was in the range of 0.0022 to 0.0026. To evaluate the effect of confinement after the spalling of the cover, M_i and M_{ACI} values are calculated with and without the top cover concrete. M_{exp} values with intact concrete cover generally represent the unconfined section capacities. Before spalling of the cover M_{exp} values are very similar to M_i values. M_{ACI} values, however, are higher (10 to 17 percent) than the experimental capacities. ACI Code's[8] stress block factors are based on normal strength concrete stress-strain curves and HSC stress-strain curves have steeper slopes for the falling branch beyond the peak.[15] This appears to be the main reason behind the overestimation of strength by ACI Code's[8] equations. After the spalling of the cover M_{exp} values represent the confined section capacities, and are 22 percent to 45 percent higher than the M_i' values without top cover. For Specimen ES-1HT strength gain due to confinement appears to be considerably high after the spalling of the top cover concrete. However, strength degradation rate in this specimen is higher than in other specimens, due to a lack of lateral support to middle longitudinal bars which resulted in poor confinement. Owing to this fact, Specimen ES-1HT was not as deformable and ductile as Specimen AS-3HT which showed the same initial strength gain after the spalling of cover concrete, and was able to maintain it for a longer time during the subsequent displacement excursions.

Equivalent plastic hinge length

Each test specimen is idealized as a cantilever column. Assuming liner elastic behavior up to the point when yielding occurs at the base of the column, the yield displacement at the tip can be computed as follows.

$$\Delta_y = \frac{\phi_y L^2}{3} \tag{2}$$

where ϕ_y is the yield curvature at the column base.

Assuming that the plastic hinge rotation at the base is concentrated at the center of the plastic hinge, and decomposing the total displacement, Δ_{max}, into two components, Δ_y and Δ_p the plastic displacement, Δ_p, can be expressed as:

$$\Delta_p = (\phi_{max} - \phi_y) L_p (L - 0.5 L_p) \tag{3}$$

Equations 2 and 3 are used for the computation of equivalent plastic hinge lengths of the specimens tested. As suggested by Khoury and Sheikh,[3] computations are performed for all the load cycles in which μ_Δ is greater than 4. Equivalent plastic hinge lengths are finally obtained by averaging the calculated plastic hinge lengths for all load cycles. Table 3 includes both experimental and predicted plastic hinge lengths for all the specimens tested. Expressions suggested by Corley[13] [$L_p = 0.20(L/d)\, d^{0.5} + 0.5d$], Mattock[13] [$L_p = 0.05L + 0.5\, d$], and Priestley and Park[14] [$L_p = 0.08L + 6d_b$] were used in this analysis. In these expressions, plastic hinge length is assumed to depend on the length of the specimen between the point of contraflexure and the section of maximum moment (L), bar diameter (d_b), and section's effective depth (d). These tests along with similar previous tests[5,6] suggest that the plastic hinge length is approximately equal to or slightly smaller than the depth of the section. The variations between the experimental lengths and values obtained from different equations suggest that a simpler expression such as $L_p = x.h$, where x can have a value between 0.9 and 1 is more appropriate.

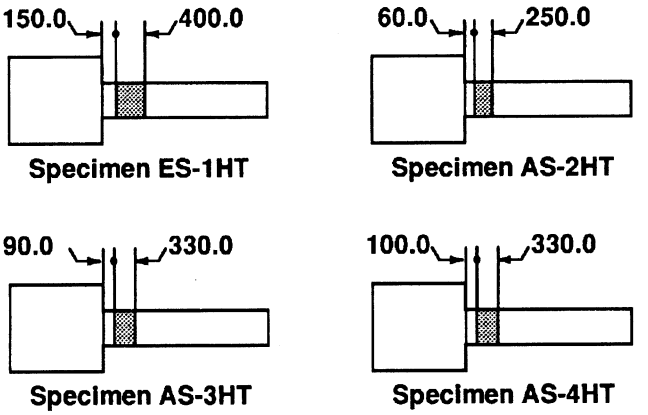

Fig. 13—Extensively damaged regions of the test specimens

Table 2—Moment capacities of specimens

Specimen	Top concrete cover in place			Top concrete cover spalled off			
	M_i	M_{ACI}	M_{exp}	M_i'	M_{ACI}	M_{exp}	M_s*
	kN.m						
ES-1HT	274	310	272	205	237	274	309
AS-2HT	287	314	286	231	260	282	323
AS-3HT	274	310	279	205	238	274	320
AS-4HT	274	310	266	204	237	296	324

* Maximum experimental moment at section adjacent to stub, as an average of both load directions

Table 3—Experimental and predicted plastic hinge length

Specimen	Length*, mm	Section depth, mm	Equivalent plastic hinge length							
			Experimental		Corley[13]		Mattock[13]		Priestley and Park[14]	
			L_p, mm	L_p/h	L_p, mm	L_p/h	L_p, mm	L_p/h	L_p, mm	L_p/h
ES-1HT	1842	305	308	1.01	247	0.81	226	0.74	265	0.87
AS-2HT	1842	305	289	0.95	248	0.81	227	0.74	265	0.87
AS-3HT	1842	305	263	0.86	248	0.81	227	0.74	265	0.87
AS-4HT	1842	305	256	0.84	247	0.81	226	0.74	265	0.87

* Length of column measured from column-stub interface to point of contraflexure

SUMMARY AND CONCLUSIONS

Four column-stub specimens made of high-strength concrete with nominal strength of 72 MPa were tested under moderate to high axial load levels and cyclic lateral displacement excursions. Results were compared with those obtained in an earlier study from similar specimens made from normal strength concrete. The following conclusions can be drawn from the work reported here.

As in NSC specimens, behavior of HSC columns subjected to constant axial load and reversed cyclic lateral load, is substantially influenced by confinement provided by rectilinear ties. HSC columns with f_c' around 72 MPa can be made to behave in a ductile manner under high levels of axial load, provided that sufficient amount of confining steel is used in an efficient configuration. Curvature ductility factors as high as 21 and displacement ductility factors as high as 7.0 were observed. Overall behavior of HSC columns was observed to be only slightly less ductile compared with that of NSC columns. However, during the stage of loading immediately beyond the peak, HSC columns displayed significantly lower deformation and energy dissipation capacities which improved during the later part of displacement excursions.

Better distribution of steel in the core and effective lateral support to the longitudinal steel bars improved the deformability and energy dissipation capacity of HSC columns significantly, as in NSC columns. The column with only four corner bars supported by tie bends showed a lack of ability to maintain moment capacity at large deformations after spalling of the cover concrete. Early buckling of middle longitudinal bars was observed, and the specimen with 13 percent more confinement steel than the Code's[8] requirements behaved in a brittle manner. There was little warning before its failure, unlike a comparable specimen in which all eight longitudinal bars were effectively supported and which was observed to be tougher and significantly more ductile.

An increase in axial load reduces column's ductility parameters and accelerates stiffness degradation with every load cycle. To compensate for this effect a larger amount of confining steel is required. Improvements in ductility, energy absorption, and dissipation capacity appear to be proportional to the increase in the amount of lateral steel, while the effect on the section moment capacity is less than proportional. When the volumetric ratio of lateral steel was kept constant, an increase in the concrete strength resulted in a less ductile behavior.

Since North American design codes' requirements for the design of confinement steel do not consider factors such as steel configuration, and level of axial load, the columns thus designed according to the code provisions can display a wide range of behavior from very ductile to brittle.

ACKNOWLEDGMENTS

Research reported here was supported by grants from the Natural Sciences and Engineering Council of Canada. The experimental work was performed in the Structure Laboratories of the University of Toronto. Technical assistance from the staff and students Jennifer Wu and Paul Eisenbach Chisholm is gratefully acknowledged.

CONVERSION FACTORS

1 inch = 25.4 mm
1 ksi = 6.895 MPa
1 kip = 4.448 kN

REFERENCES

1. Paulay, T., "Seismic Design of Ductile Moment Resisting Reinforced Concrete Frames, Columns: Evaluation of Actions," *Bulletin of the New Zealand National Society for Earthquake Engineering*, Vol. 10, No. 2, June 1977, pp. 85-94.

2. Bayrak O., "High Strength Concrete Columns Subjected to Earthquake Type Loading," M.A.Sc. Thesis, Department of Civil Engineering, University of Toronto, Toronto, Ontario, 1995, 239 p.

3. Khoury, S. S., and Sheikh, S. A., "Behavior of Normal and High Strength Confined Concrete Columns with and without Stubs," *Research Report* No. UHCEE 91-4, Department of Civil and Environmental Engineering, University of Houston, Texas, Dec. 1991, 345 p.

4. Sheikh, S. A., and Uzumeri, S. M., "Strength and Ductility of Tied Concrete Columns," *Journal of the Structural Division*, ASCE, V. 106, ST5, May 1980, pp. 1079-1102.

5. Sheikh, S. A., Khoury, S. S., "Confined Concrete Columns with Stubs," *ACI Structural Journal*, V. 90, No. 4, July-Aug. 1993, pp. 414-431.

6. Sheikh, S. A.; Shah, D. V.; and Khoury, S. S., "Confinement of High-Strength Concrete Columns," *ACI Structural Journal*, V. 91, No. 1, Jan.-Feb. 1994, pp. 100-111.

7. Sheikh, S. A., and Toklucu, M. A., "Reinforced Concrete Columns Confined by Circular Spirals and Hoops," *ACI Structural Journal*, V. 90, No. 5, Sept.-Oct. 1993, pp. 542-553.

8. ACI Committee 318, *Building Code Requirements for Reinforced Concrete and Commentary (ACI 318-89/ACI 318R-89)*, American Concrete Institute, Detroit, 1989, 353 p.

9. *Code for Design of Concrete Structures for Buildings (CAN3-A23.3-M94)*, Canadian Standards Association, Rexdale, Ontario, 1994, 199 p.

10. *Code of Practice for the Design of Concrete Structures*, (NZS 3101:1982), Standards Association of New Zealand, Wellington, 1982, Part 1, 127 p., and Part 2, 156 p.

11. Sheikh, S. A., "Design of Confinement Steel for Reinforced Concrete Columns," 5th U.S. National Conference on Earthquake Engineering, Chicago, July 10-14 1994, V. 2, pp. 609-618.

12. Ehsani, M. R., and Wight, J. K., "Confinement Steel Requirement for Connection in Ductile Frames," *Journal of Structural Division, ASCE,* V. 116, ST 3, Mar. 1990, pp. 751-767.

13. Corley, W. G., "Rotational Capacity of Reinforced Concrete Beams," ASCE, *Proceedings*, V. 92, ST 5, Oct. 1966, pp. 121-146.

14. Priestley, M. J. N., and Park, R., "Strength and Ductility of Concrete Bridge Columns Under Seismic Loading," *ACI Structural Journal*, V. 84, No. 1, Jan.-Feb. 1987, pp. 69-76.

15. Collins, M. P., and Mitchell D., *Prestressed Concrete Structures*, Prentice-Hall, Englewood Cliffs, New Jersey, 1991, 766 p.